

Voronoi Diagrams and Morse Theory of the Distance Function

Dirk Siersma

June 28, 1996

Abstract

We consider the (minimal) distance function of a point in the plane to a set \mathcal{P} of N points in the plane. The locus of non-differentiability of this distance function consists (besides of the points of \mathcal{P}) exactly of the Voronoi diagram of \mathcal{P} . We show that the number of minima (m), maxima (M) and ‘saddle points’ (s) of the distance function satisfy:

$$m - s + M = 1$$

This is similar to the Morse type of statements for differentiable functions.

The saddle points occur exactly where a Delaunay edge cuts the corresponding Voronoi edge in its interior. The set of those edges form a subgraph of the Delaunay graph, which connects all minima and saddle points. This graph divides the plane into regions. In each of the compact regions, there is exactly one maximum, the non compact regions don't contain a local maximum.

At the end we classify all those graphs if \mathcal{P} contains of 3 or 4 points.

Introduction

Given a set of N different points $\mathcal{P} = \{P_1, \dots, P_N\}$ in the plane \mathbb{A}^2 we consider the *Voronoi diagram* of the Euclidean distance function d :

$$\mathbb{V}D(\mathcal{P}) = \{X \in \mathbb{A}^2 \mid \exists i \neq j \text{ such that } \forall k \ d(X, P_i) = d(X, P_j) \leq d(X, P_k)\}.$$

The (*closed*) *Voronoi cells* are defined by:

$$\mathbb{V}C(P_i) = \{X \in \mathbb{A}^2 \mid \forall k \ d(X, P_i) \leq d(X, P_k)\}.$$

For the theory of Voronoi diagrams we refer to Aurenhammer [Au], Edelsbrunner [Ed] and the book of Okabe-Books-Sigihara [OBS]. Voronoi diagrams have many applications in mathematics and computer science, but also in geography, biology, cristallography, marketing, cartography, etc.

Consider the N distance functions

$$d_k(X) = d(X, P_k)$$

A natural function to study is $d(X) = \min\{d_1(X), \dots, d_N(X)\}$. In order to have differentiability in the points of \mathcal{P} and to have a nicer formula for the gradient, we study

$$D(X) = \min\{d_1^2(X), \dots, d_N^2(X)\},$$

which behaves the same, e.g. D and d have the same set of level curves, minima, maxima and ‘saddle points’. Remark that $D(X) = d_i^2(X)$ on $\text{VC}(P_i)$. The function D is differentiable on the interior of all the Voronoi cells. The restriction of D to a closed Voronoi cell $\text{VC}(P_i)$ is differentiable and on this set

$$\text{grad } D(X) = \text{grad } d_i^2(X) = 2XP_i$$

It follows that the set of points where D is not differentiable is exactly $\mathbb{V}D(\mathcal{P})$.

The level curves of the distance function d can be considered as *wave fronts*, which start from the points of \mathcal{P} . These wave fronts $\{d = \epsilon\}$ bound sets $\{d \leq \epsilon\}$, where the wave front already passed, just as an region passed by a forest fire.

The change of topology of these regions $\{d \leq \epsilon\}$ is studied in this paper. We first consider an instructive example with 3 points, where two different positions of the points of \mathcal{P} give rise to different topological behaviour. An indicator for topological changes is the Euler characteristic χ .

At the beginning the wave fronts surround three different regions. So the Euler characteristic $\chi = 3$. We’ll report about the changes in χ . Next two regions meet in a common point and we get two contractible regions, so $\chi = 2$. After that the third region meets the other (combined) region, this gives $\chi = 1$.

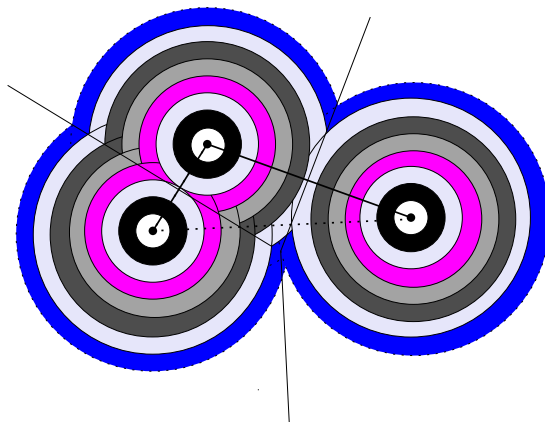


Figure 1: evolution of a wave front from three points, case A

In case A (figure 1), where one of the angles is obtuse, this region becomes bigger and bigger and χ does not change anymore.

In case B (figure 2) all the angles are sharp and now the wave fronts meet another time and enclose a region in the middle. The set $\{d \leq \epsilon\}$ is ‘circular’ and no longer contractible. Now $\chi = 0$.

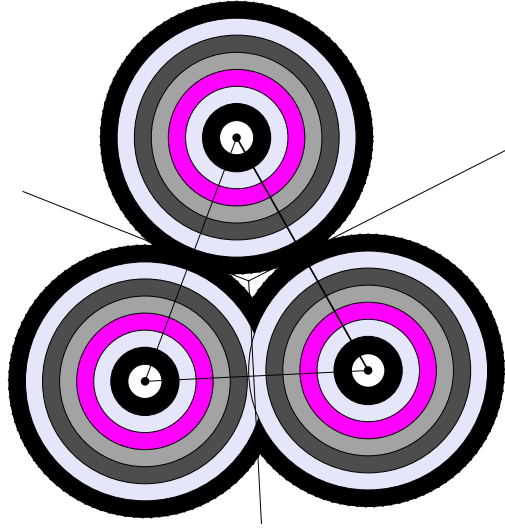


Figure 2: evolution of a wave front from three points, case B

If one goes on then the enclosed region in the middle disappears and this changes χ to 1. There is only one region left, which is contractible and there are no changes if ϵ increases more.

We intend to study this type of process in the paper. The special points, where the wave fronts meet and the points, where they become non-differentiable, are directly related to the Voronoi diagram. As we see in the above example we need more refined information than the Voronoi diagram in order to understand the topological behaviour of the wave fronts.

Behaviour of D on the plane \mathbb{A}^2 .

The behaviour of D on the *interiors of the Voronoi cells* is clear. In the points of \mathcal{P} the function D has its minimal value and there are no other critical point in the interior of the Voronoi cells.

Next we study the neighborhoods of the points A on the Voronoi diagram.

Let $e_{ij} = \text{VC}(P_i) \cap \text{VC}(P_j)$ be a Voronoi edge between the Voronoi cells of P_i and P_j . Let m_{ij} be the perpendicular bisector of $P_i P_j$ and $Q_{ij} = m_{ij} \cap P_i P_j$. The edge $e_{ij} \subset m_{ij}$. The position of Q_{ij} with respect to e_{ij} is important. There are three cases (cf figure 3):

1. Q_{ij} lies outside e_{ij} ,
2. Q_{ij} lies in the interior of e_{ij} ,
3. Q_{ij} is a boundary point of e_{ij} .

In cases (1) and (3) D is monotone on the edge; in case (2) D is not monotone, but increasing from Q_{ij} in both directions.

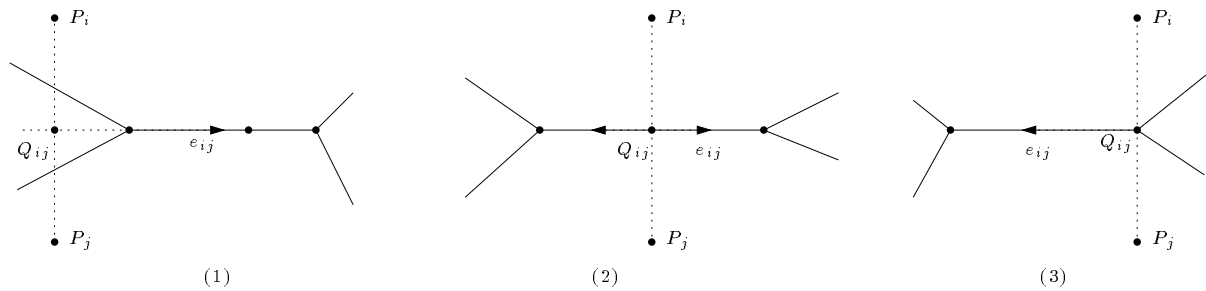


Figure 3: positions of $P_i P_j$ with respect to e_{ij}

Consider a point A on the *interior* of a Voronoi-edge $e_{ij} = \mathbb{V}C(P_i) \cap \mathbb{V}C(P_j)$.

If A is different from the center of the line $P_i P_j$ then there is no change in the topology of the lower level sets $\{d \leq \epsilon\}$, since the set of level curves of D is topological equivalent to a set of parallel lines, More precisely: there exist a homeomorphism ϕ of a open neighborhood of A onto an open set in \mathbb{R}^2 such that the composed function $D\phi$ is a linear function. In this case we call A a *topological regular point* of D (figure 4).

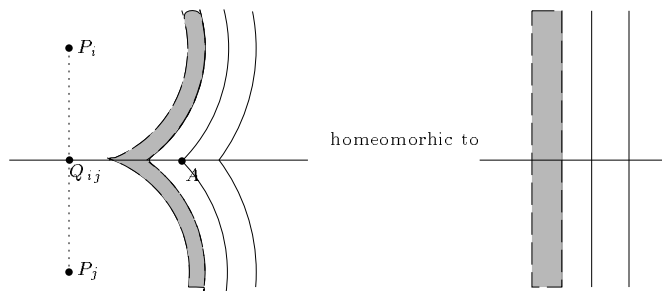


Figure 4: topological regular situation

If A coincides with Q_{ij} , the center of the line $P_i P_j$, then it is possible to make a non-differentiable (but homeomorphic) change of coordinates ϕ , such that the composed function $D\phi$ is given by the formula: $c_A + x^2 - y^2$, which defines a differentiable saddle point.

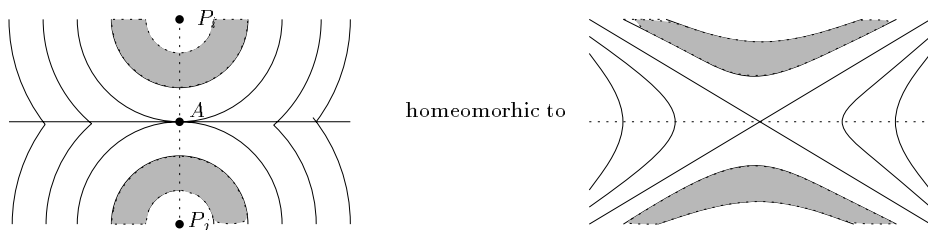


Figure 5: a topological saddle point

In this case we call A a *topological saddle point* of D (figure 5).

The remaining points to consider are the *vertices of the Voronoi diagrams*. We consider the following cases, related to the behaviour of the restriction of D to the edges of the Voronoi diagram which contain A (figure 6)

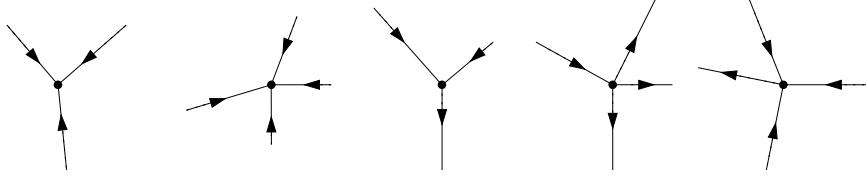


Figure 6: situation near Voronoi vertices

i) A is a maximum of this restriction. We can now use a non-differentiable (but homeomorphic) change of coordinates ϕ , such that the composed function $D\phi$ is given by the formula: $c_A - x^2 - y^2$, which defines a *local maximum* of D (figure 7).

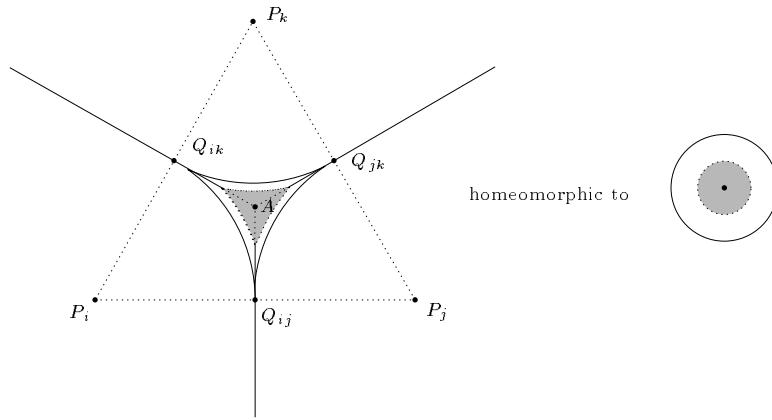


Figure 7: a topological maximum

ii) A is a maximum on all but one of the adjacent edges. Also in this case there is a non-differentiable (but homeomorphic) change of coordinates such that D is equivalent to a linear function. We call A again a *topological regular point* of D (figure 8).

(iii) Other cases don't exist:

Consider a multiple point A of multiplicity $m \geq 3$. There exists a circle C with center A through m points of \mathcal{P} , which contains (by the empty circle criterium) no other points of \mathcal{P} on C in its interior. Assume that those points on the circle are numbered P_1, \dots, P_m in clockwise order. We denote $P_0 = P_m$. We consider the arcs $\angle P_{i-1}P_i$ and denote the middle of this arc by R_{i-1} . The disc bounded by C is divided into m sectors $AP_{i-1}P_i$ (cf. figure 9).

If $\angle P_i P_{i+1} < \pi$ then it follows that the intersection points Q_i of the middle perpendicular m_i of $P_i P_{i+1}$ lies in the sector $AP_i P_{i+1}$. Therefore we know that on the interval $R_i A$ the function D is increasing, so maximal at A . So if all arcs are smaller than π then we have this increasing behaviour on all the Voronoi edges, which are adjacent to A , so D is maximal at A (case (i)).

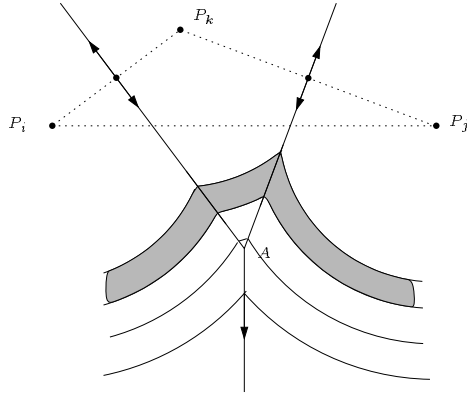


Figure 8: A vertex, which is topological regular

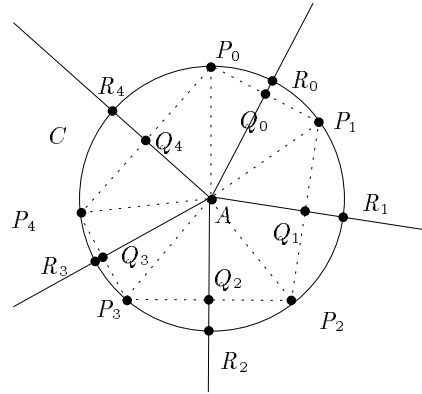


Figure 9: case i

If one arc (say $\angle P_m P_1$) is greater or equal than π (figure 10), then all the others are smaller than π . The point Q_0 is not contained in the sector $AP_0 P_1$ so does not lie on $R_0 A$. Therefore we know that on the interval $R_0 A$ the function D is decreasing, so minimal at A . On all the other intervals $R_i A$ the function D is increasing, so maximal at A . So we are in case (ii).

NB. Remark that the points Q_i are not necessarily on the Voronoi edges. We know only that this edges occur in a neighborhood of A , since other points P_* from \mathcal{P} can influence the end points of the Voronoi edge, cf. figure 11. By the empty circle criterium P_* must be outside C , so one end point must be A and the other lies somewhere on the half-ray from A trough R_i (including infinity).

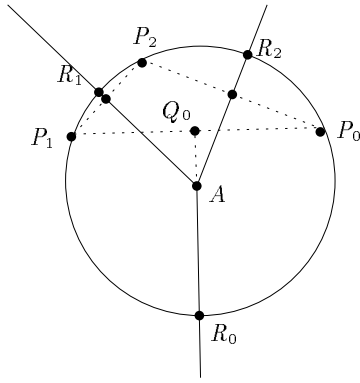


Figure 10: case ii

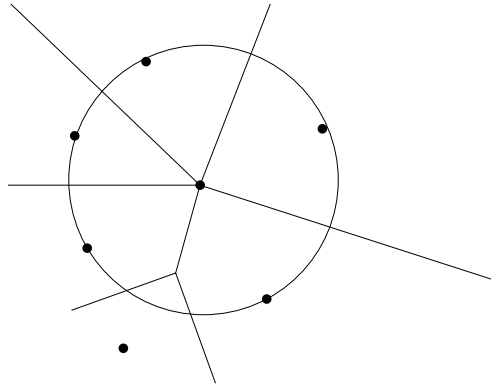


Figure 11: the influence of an other point

Main Theorem

Theorem *Let m , s and M be respectively the number of (topological) minima, saddle points and maxima of the distance function D . We have:*

$$m - s + M = 1$$

For the proof we use the framework of Morse theory, which is well known in differential topology. See Milnor [Mi], Hirsch [Hi], etc and its generalizations to stratified spaces by Goresky and MacPherson [GM].

Definition The minima, the saddle points and the maxima of D are called critical points of index 0, 1, 2 respectively. The corresponding values are called critical values. The other points are called (topologically) regular.

We have the following types:

a) differentiable regular points in the interior of the Voronoi cells,

- b) topological regular points, which lie on the interior of certain edges,
- c) topological regular points, which are multiple points.

We formulate now the main

Assertion \mathbb{A}^2 has the homotopy type of a finite CW-complex, with one λ -cell for each critical point of index λ . So if μ_λ denotes the number of cells of index λ then:

$$\mu_0 = m = N ; \quad \mu_1 = s ; \quad \mu_2 = M$$

Here a 0-cell is a point, a 1-cell an interval and a 2-cell a disc. The Euler-characteristic is a homotopy invariant and it can be computed from the cell complex as alternating sum of the number of cells of increasing dimension. So:

$$1 = \chi(\mathbb{A}^2) = \mu_0 - \mu_1 + \mu_2$$

There are 3 steps in the proof of the assertion:

1. Regular interval theorem:

Let $[a, b]$ be an interval, which contains no critical value of D , then

- $D^{-1}[a, b]$ is homeomorphic to the product $D^{-1}(a) \times [a, b]$
- the set $D^b := D^{-1}[0, b]$ is homotopy equivalent to D^a .

2. Passage through a critical level:

Let c be a critical value of D , and $[a, b]$ an interval around c , containing no other critical values. There holds:

The set D^b is homotopy equivalent to $D^{-1}(a) \cup_\phi F$. where F is a set of cells, containing a λ -cell for each critical point of index λ in $D^{-1}[a, b]$, each cell attached to D^a separately by the map ϕ .

3. Third step

We use the first two steps in order to determine the homotopy type of D^b until b greater than the maximal critical value of D . Finally we show that \mathbb{A}^2 and D^b are homotopy equivalent.

About the proofs:

The main ingredient is the construction of a vectorfield \mathbf{w} on almost all of \mathbb{A}^2 . The induced flow ψ_t is supposed to send level sets into level sets, such that:

$$D(\psi_t(X)) - D(X) = t.$$

For a differentiable function $f : \mathbb{A}^2 \rightarrow \mathbb{R}$ we can construct such a flow as soon as f is a submersion (i.e. $\text{grad} f \neq 0$) by lifting the vectorfield $\frac{d}{dt}$ on \mathbb{R} . There is a lot of freedom: we can lift $\frac{d}{dt}$ to

all directions, except the tangent directions to the level curves. A natural choice is the gradient direction and then

$$\mathbf{w} = \frac{\text{grad}f}{\|\text{grad}f\|^2}$$

lifts $\frac{d}{dt}$.

Of course near a critical point of f we cannot do this, but there we'll consider locally cell-attaching.

In our case D is not differentiable on $\mathbb{V}D(\mathcal{P})$, so we have to pay extra attention to a small neighborhoods of the Voronoi diagram.

Proof of the regular interval theorem:

We define the vectorfield \mathbf{w} on open sets of $D^{-1}[a, b]$ and glue them later with the help of a partition of unity.

a) On interior points, different from P_i of $\mathbb{V}C(P_i)$ we define

$$\mathbf{w} = \frac{\text{grad}f}{\|\text{grad}f\|^2}$$

b) Near Voronoi edges e_{ij} and away from the saddle points and multiple points we define \mathbf{w} parallel to this edge as lift of $\frac{d}{dt}$ (figure 12),

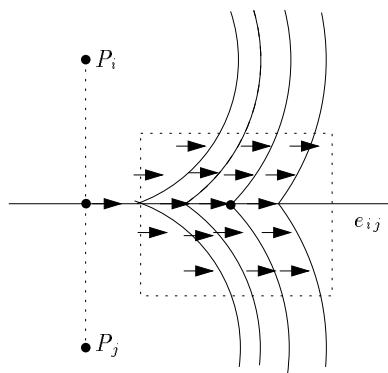


Figure 12: near regular points on the edges

The level curves fail to be transversal to the e_{ij} -direction only on the line through P_iP_j and we can assume that this line is outside our neighborhood, since we avoid saddles.

c) Near multiple points A , which are topologically regular, we proceed as follows. First remember that there must be one arc between two consecutive directions AP_i and AP_j , which is greater or equal to π . Assume first that this arc is greater than π . It follows that P_iP_j does not contain A and passes ‘above’ A in figure 13.

Choose a small neighborhood of A , which avoids P_iP_j . Let e_{ij} be the outgoing edge. We define \mathbf{w} parallel to this edge as lift of $\frac{d}{dt}$. Remark that this causes a discontinuity of the vectorfield on

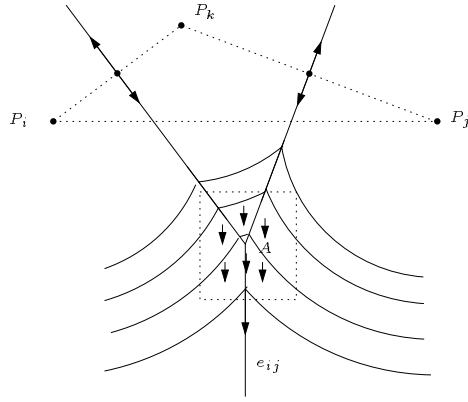


Figure 13: case c

the Voronoi edges, since the normalization on each of the Voronoi cells is different. Nevertheless the induced flow is continuous.

The level curves in $\mathbb{V}C(P_i)$ and $\mathbb{V}C(P_j)$ are never tangent to the e_{ij} -direction (this happens only in points of the line P_iP_j). In the other adjacent cells $\mathbb{V}C(P_k)$ this non-transversality can only happen on the perpendicular from P_k to the e_{ij} -direction, and this can be assumed to be outside our neighborhood.

In the ‘missing’ case, where the arc is equal to π , we have to be more carefull (figure 14).

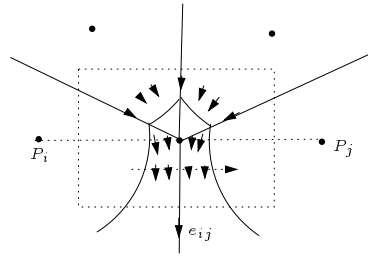


Figure 14: case c with one angle π

We have to interpolate between the radial vectorfield in the ‘upper’ half of the disc and the ‘vertical’ direction (parallel to e_{ij}) in such a way that we avoid tangencies on (and ‘above’) P_iP_j . The ‘vertical’ direction can only be attained on a ‘lower’ part of the neighborhood.

At the end we glue all the vectorfields with a partition of unity. The resulting vectorfield \mathbf{w} defines a flow such that points in $D^{-1}[a, b]$ flow during the time $t = D(X) - a$ to $D^{-1}(a)$. The rest of the proof continues as in the differentiable case: this flow and the flow lines induce the product structure and the homotopy equivalence.

Proof of the passage through the critical level

We have to consider three kinds of topological critical points: minima, saddles and maxima.

- a) The minima are attained exactly in the points of \mathcal{P} , the minimal value is 0.
 $D^a = \emptyset$ if $a < 0$, $D^{-1}(0) = \{P_1, \dots, P_N\}$, and D^b is for b small enough a set of disjoint discs. So we start with a set of points $D^0 = \{P_1, \dots, P_n\}$ (0-cells) and D^b has the same homotopy type if b is small enough.
- b) Let A be a saddle point and $D(A) = c$. We consider a small neighborhood U of A . Let $c_- < c < c_+$ arbitrary near to c .

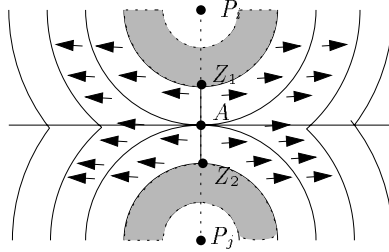


Figure 15: attaching a 1-cell

Let the level curve with value c_- cuts $P_i P_j$ in the points Z_1 and Z_2 . We have locally:

$$D^{c_-} \cup [Z_1 Z_2] \simeq^h D^{c_+}$$

or

$$(U \cap D^{c_-}) \cup [Z_1 Z_2] \simeq^h U \cap D^{c_+}$$

This means that a 1-cell (interval) $Z_1 Z_2$ is attached to D^{c_-} . The homotopy equivalence (\simeq^h) is induced by the vectorfield parallel to the edge e_{ij} , normalized properly (figure 15).

- c) Let A be a maximum with level c . We consider again a small neighborhood U and levels $c_- < c < c_+$ arbitrary near to c .

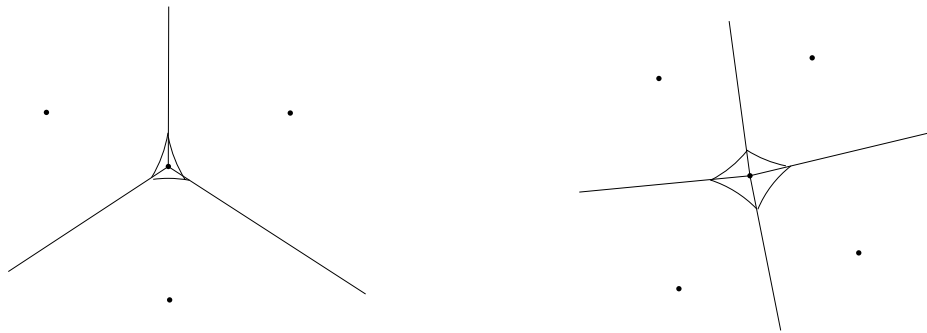


Figure 16: attaching a 2-cell

The level curve with value c_- consists of circular arcs, defining a simple closed curve around A , which bounds a topological disc F_2 (figure 16). So locally:

$$D^{c_+} = D^c \simeq^h D^{c_-} \cup F_2$$

or

$$U \cap D^{c+} = U \cap D^c \simeq^h (U \cap D^{c-}) \cup F_2$$

where F_2 is a 2-cell.

Next we ‘globalize’ within $D^{-1}[a, b]$. Let c be a critical value, which corresponds to critical points of index 1 or 2 and consider levels $c_- < c < c_+$ as before. Use outside the chosen neighborhoods of the critical points the vectorfield \mathbf{w} as defined in the proof of the regular interval theorem and glue it with a gradient type of vectorfield near the saddlepoint, where a 1-cell $Z_1 Z_2$ is attached.

After integrating this vectorfield we get

$$D^{c+} \simeq^h D^{c-} \cup F$$

where F denotes the corresponding cells of index 1 or 2. Next use the general interval theorem (as in Milnor’s situation):

$$D^b \simeq^h D^{c+} \simeq^h D^{c-} \cup F \simeq^h D^a \cup F$$

The third step

We start with $c = 0$: D^0 is a set of N 0-cells. Next we move c from 0 to infinity and add the cells mentioned above as soon as we pass through a critical level. We do this until we have reached a value b , which is greater than the maximal critical value.

Although the interval $[b, \infty)$ is not bounded, we can still use a regular interval theorem, since the map:

$$D^{-1}[b, \infty) \rightarrow [b, \infty)$$

is proper. This means that the inverse image of a compact set is again compact. This is clear in our case since $D^{-1}[0, z]$ is always bounded.

Now we have finished the proof of the main theorem.

Graphs

The Delaunay graph related to the set of points \mathcal{P}

The vertices of the *Delaunay graph* $Dl(\mathcal{P})$ are the points of \mathcal{P} . The graph contains an edge connecting two points of \mathcal{P} if and only if their Voronoi cells share a common edge. In terms of the point set \mathcal{P} the graph $Dl(\mathcal{P})$ can be defined by the ‘empty circle criterium’. Consider triangles or polygons with vertices from \mathcal{P} on the circumcircle and no points of \mathcal{P} in its interior. The edges of these triangles or polygons are just the edges of the Delaunay graph of \mathcal{P} . Note that we have made no genericity assumptions. The Voronoi diagram and the Delaunay graph are duals in a graph theoretical sense (at least for the bounded pieces of the Voronoi diagram).

The sm-graph related to the set of points \mathcal{P}

We define the following graph $sm(\mathcal{P})$:

- the vertices are the points of \mathcal{P} . They correspond to the minima of D .
- the edges are those line segments P_iP_j which intersects the Voronoi edge e_{ij} in its interior. These edges correspond 1-1 with the saddles of D , via the intersection points $Q_{ij} = P_iP_j \cap e_{ij}$.

We call this graph the *saddle-minima graph* of \mathcal{P} , for short $sm(\mathcal{P})$ (cf figure 17).

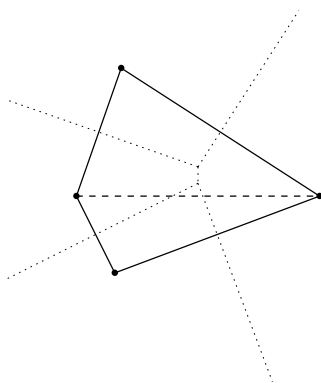


Figure 17: saddle minimum graph

This graph coincides with the *Gabriel graph* $Gb(\mathcal{P})$, cf [GS], [Ur]. This Gabriel graph has again the points of \mathcal{P} as vertices, but the edges correspond to those P_iP_j such that the closed disc with P_iP_j as diameter contains no other points of \mathcal{P} . In the recent reference work [OBS] the Gabriel graph is defined with the interior of the disc. With that definition of $Gb(\mathcal{P})$ there exist examples where $sm(\mathcal{P})$ and $Gb(\mathcal{P})$ are different. This happens e.g. when the triangle $P_iP_kP_j$ has a right angle in P_k (cf figure 18). Aurenhammer [Au] is not clear about this point.

Properties of $sm(\mathcal{P})$:

1. $sm(\mathcal{P})$ is a subgraph of the Delaunay graph.

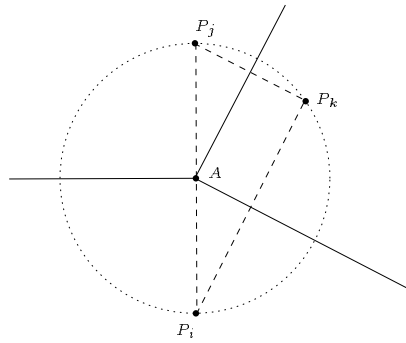


Figure 18: A right angle

2. $sm(\mathcal{P})$ is connected

This follows from the fact that a wave front, starting in P_i must meet the union of the wave fronts from the other points of \mathcal{P} in an arc, which belongs to a circle around one of the points, say P_j (cf. figure 19).

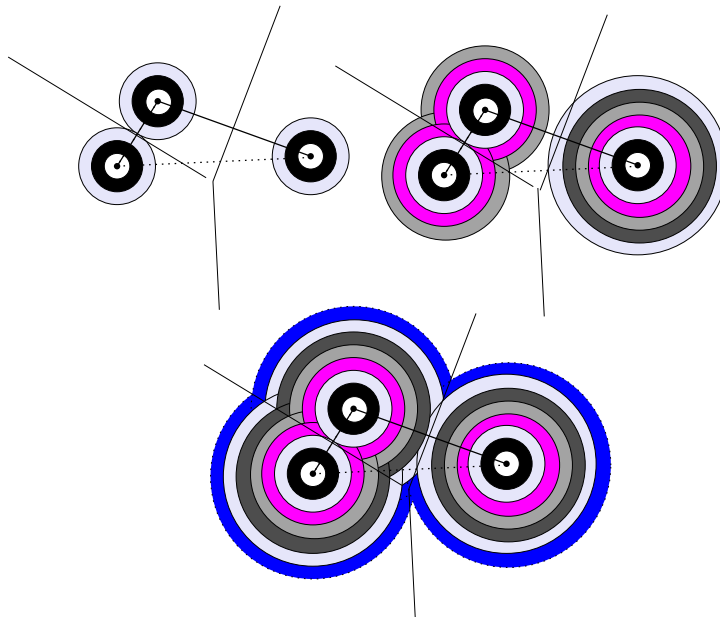


Figure 19: all wave fronts connect

3. $sm(\mathcal{P})$ is a subgraph of $Gb(\mathcal{P})$,

The saddle-minimum graph is important since it contains all ‘minimal’ distances between ‘obstacles’ P_1, \dots, P_N . This seems to be useful for movements of robots, ships, etc.

Next apply Eulers formula:

$$V - E + R = 1$$

to $sm(\mathcal{P})$, where:

- the number of vertices $V = m$, the number of minima of D ,
- the number of edges $E = s$, the number of saddles of D ,
- R is the number of bounded regions, defined by the graph

Proposition *The number of bounded regions, defined by $sm(\mathcal{P})$ is equal to M , the number of maxima of D . In fact in each region there is exactly one maximum in the interior.*

Proof We have

$$R = 1 - V + E = 1 - m - s = M$$

due to the main theorem of this paper. Moreover consider a region, defined by $sm(\mathcal{P})$, then each edge contains a saddle point. From the edges to the inside of the region the function D is increasing. In each region there must be at least one maximum, so exactly one. \square

The Voronoi diagram with extra structure

The Voronoi diagram $\mathbb{V}D(\mathcal{P})$ can be considered as a planar graph with some extra infinite edges. (One can also compactify by adding one point at infinity and gets in that way a graph on the sphere). While considering the behaviour of the distance function we can give this graph some extra structure. First one can add the saddle points to the graph and next one can put arrows in the direction of increasing D . This directed graph, the enriched Voronoi diagram, contains all information for the topological study of this paper (figure 20).

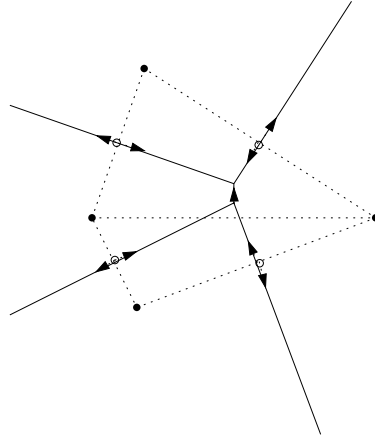


Figure 20: enriched Voronoi diagram

Configurations with 3 or 4 points

In this section we list generic configurations with 3 or 4 points. We classify them with respect to the inclusion $sm(\mathcal{P}) \subset Dl(\mathcal{P})$.

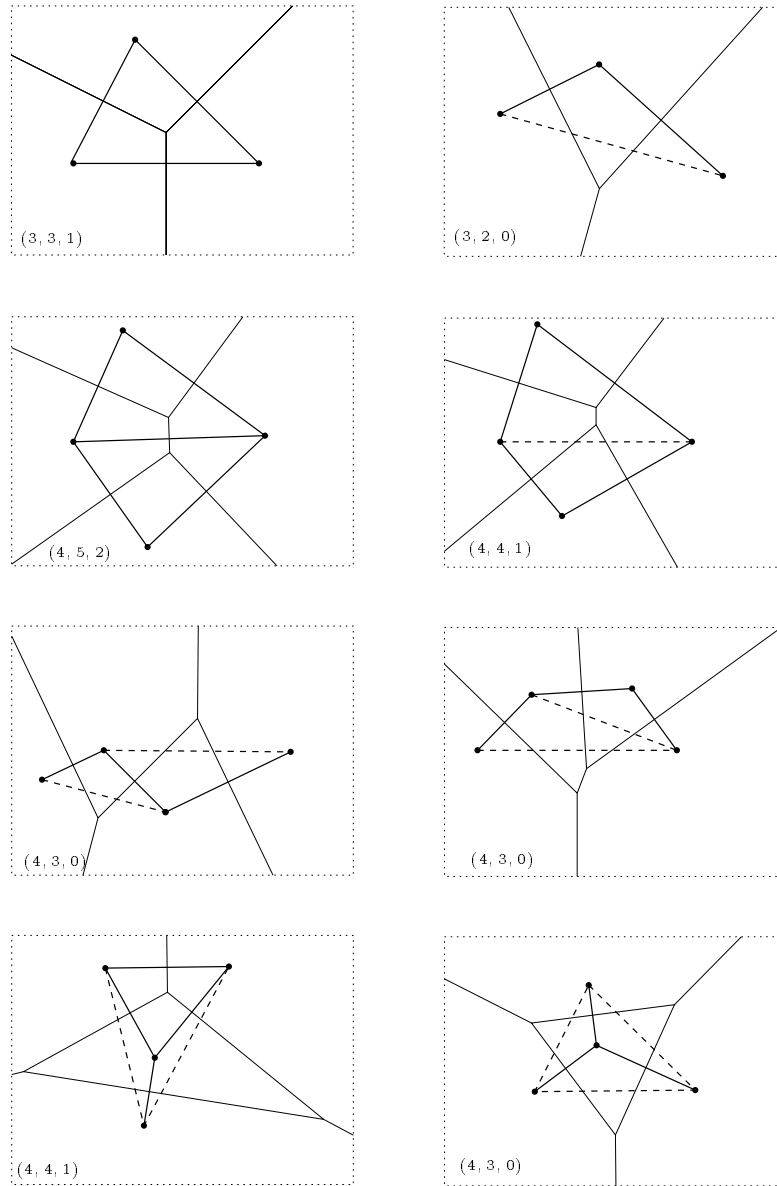


Figure 21: generic configurations with 3 or 4 points

The edges of $Dl(\mathcal{P})$, which are not contained in $sm(\mathcal{P})$ are dashed in figure 21. The notation (m, s, M) refers to the number of minima, saddles and maxima.

Remarks and Questions

Most of the theory of this paper can be generalized to other distance functions and to higher dimensions. We discuss here only some examples.

Johnson-Mehl models

In this model one considers weighted distance functions

$$d^*(X, P_k) = w_k d(X, P_k) \text{ with } w_i > 0$$

and d the usual Euclidean distance.

For two point sites P_1, P_2 the conflict set is

- a circle if $w_i \neq w_j$
- a line if $w_i = w_j$

In our Morse theoretic approach, we start with two wave fronts originating from P_1 and P_2 with different ‘speeds’ w_1 and w_2 (figure 22).. The corresponding function d (the minimum of the distance functions) has a minimum at the points P_1 and P_2 , a saddle point in a point Q on P_1P_2 . This point is the intersection of the conflict set with P_1P_2 . All other points are topological regular, even the other intersection point of the conflict set with the line through P_1P_2 .

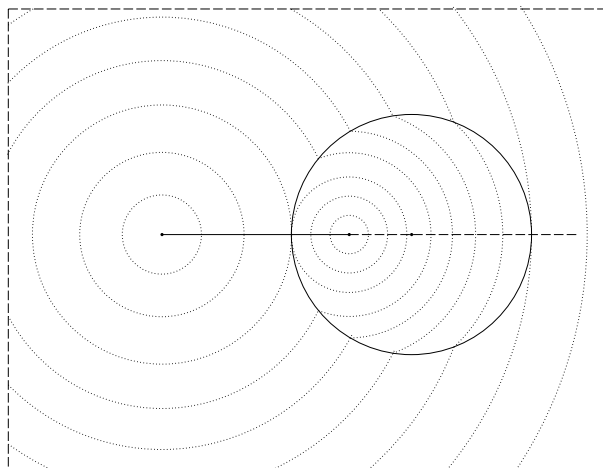


Figure 22: Johnson-Mehl with two points

We calculate again the alternating sum of the indices of the critical points:

$$\mu_0 - \mu_1 + \mu_2 = 2 - 1 + 0 = 1$$

We show in the next pictures, figures 23 and 24 two situations with three points:

$$\text{In these cases } \mu_0 - \mu_1 + \mu_2 = 3 - 3 + 1 = 1 \text{ and } \mu_0 - \mu_1 + \mu_2 = 3 - 2 + 0 = 1$$

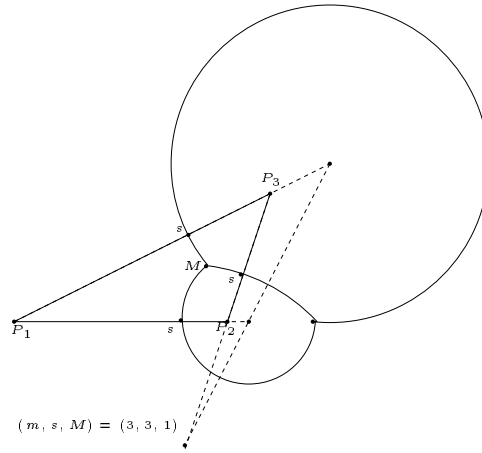


Figure 23: Johnson-Mehl with three points

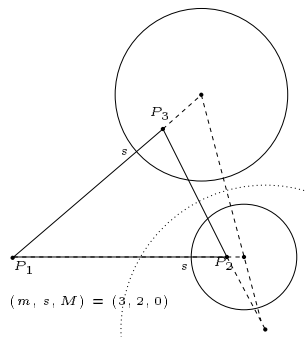


Figure 24: Johnson-Mehl three points

Remark, that the centers of the three conflict circles are on a line.

N.B. We don't claim that these are all possibilities with 3 points.

Convex sites

Let now \mathcal{P} be a collection of compact convex subsets in the plane. These situation occurs in several papers in computational geometry. It seems to be an accepted result, that in these case the conflict set of two general convex sites is a differentiable curve and that the distance functions to each of the sites are differentiable. AI could not find a mathematical rigorous reference in the literature. An elementary geometrical proof was communicated to me by Goddijn [Go].

Next we show in three examples, each consisting of three convex sites the behaviour of the minimal distance function d (figure 25) The third example frtom [VFOR] does not occur in the cases of point sites.

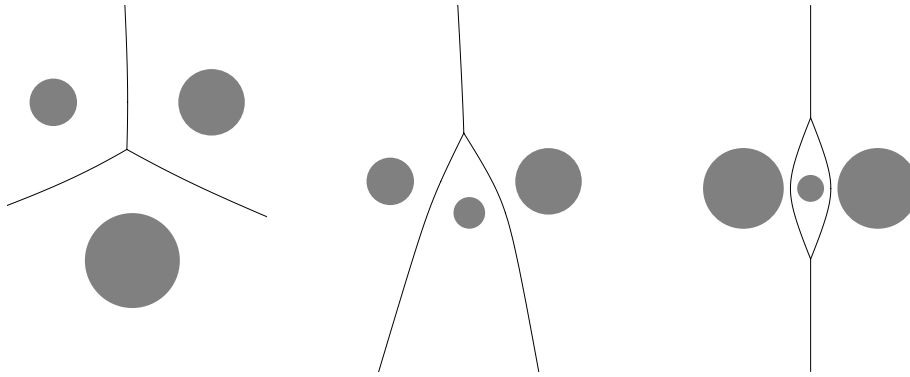


Figure 25: Voronoi diagrams for three convex sets

Piece-wise linear distance functions

In [LS] one considers a convex set B together with a point O , arbitrarily chosen and fixed in the interior of B . We will refer to the position of B in the plane in which O lies at the origin as the *standard position* of B and denote by B_0 the set of points of B when given that standard position. One defines the B -distance between two points P and Q in the plane as

$$d_B(P, Q) = \inf \{ \lambda : Q \in P + \lambda B_0 \}.$$

This distance function is always finite and continuous, obeys the triangle inequality but need not necessarily be symmetric.

For more details see [Lay]

In case B is a polygonal object then the conflict sets consists of polygonal arcs. This also true if one considers convex polygonal sites in stead of points.

We give some examples (figures 26 and 27) where one considers again the behaviour of the B -type wave fronts, originating from some point sites.

Also here we see ‘Morse-type’ singular points.

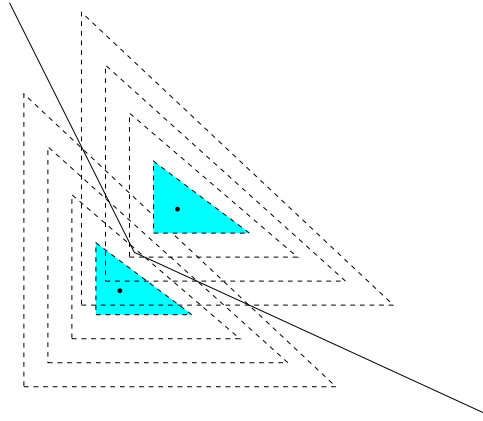


Figure 26: PL with 2 points

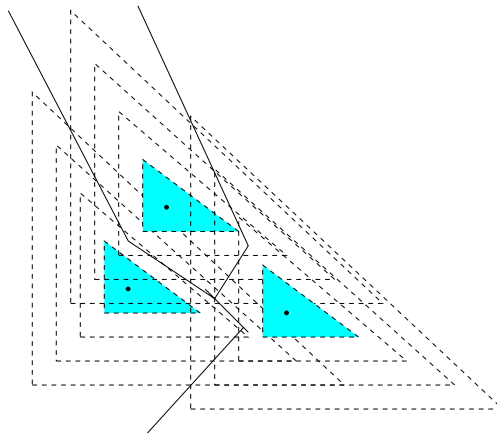


Figure 27: PL with 3 points

Generalization to higher dimensions

The definitions of Voronoi diagram, Voronoi cell and the distance square function D generalize to higher dimensions without problem.

Let now $\mathcal{P} = \{P_1, \dots, P_N\}$ be a set of points in an n -dimensional affine space \mathbb{A}^n .

The Voronoi diagram is a stratified set (which consists of a union of smooth strata). In a generic situation strata of codimension k correspond to the intersection of k closed Voronoi cells. In a non-generic situation more than k cells can intersect in a stratum of codimension k (e.g. if 4 points are on a circle in the plane).

We indicate some examples, which show the Morse theoretic approach in this case. We restrict to 3 dimensions. We denote by $\Delta\chi$ the increase in Euler characteristic. Typical Morse changes in lower level sets $\{d \leq \epsilon\}$ are:

- For a minimum: adding of a 0-cell, $\Delta\chi = 1$, just as for $f = x^2 + y^2 + z^2$,
- For a saddle point there are two possibilities:
 adding a 1-cell, $\Delta\chi = -1$, just as for $f = x^2 + y^2 - z^2$,
 adding a 2-cell, $\Delta\chi = +1$, just as for $f = x^2 - y^2 - z^2$,
- For a maximum: adding a 3-cell, $\Delta\chi = -1$, just as for $f = -x^2 - y^2 - z^2$

We call them respectively critical points of index 0, 1, 2 and 3. The corresponding number of critical points is denoted by $\mu_0, \mu_1, \mu_2, \mu_3$.

All these changes occur (in a topological way) in the next examples.

Example Three points in \mathbb{A}^3 .

The three point form a triangle in the plane. If the triangle is sharp then the lower level sets $\{d \leq \epsilon\}$ start with 3 balls, $\chi = 3$; next these balls consecutive connect in the centers of the edges P_iP_j to a ‘necklace’, $\chi = 3 - 3 = 0$. Then the ‘hole’ in the middle of the necklace is filled by a 2-cell, $\chi = 0 + 1 = 1$ and after that there are no more jumps in the topology and the lower level sets fill the whole \mathbb{A}^3 . About the critical points:

index 0 at the three vertices,

index 1 at the three centers of the edges,

index 2 at the center of the circumcircle,

no points of index 3.

$$\mu_0 - \mu_1 + \mu_2 - \mu_3 = 3 - 3 + 1 - 0 = 1.$$

If the triangle is obtuse then the lower level sets $\{d \leq \epsilon\}$ start again with 3 balls, $\chi = 3$; next these balls consecutive connect in the midpoints of the two of the edges P_iP_j to a ‘chain’, $\chi = 3 - 2 = 1$. After that there are no more jumps in the topology and the lower level set fill the whole \mathbb{A}^3 . About the critical points:

index 0 at the three vertices,

index 1 at the the midpoints of two edges,

no points of index 2 ,

no points of index 3.

$$\mu_0 - \mu_1 + \mu_2 - \mu_3 = 3 - 2 + 0 - 0 = 1.$$

Example Four points in \mathbb{A}^3 .

We suppose that the points form a regular tetrahedron, or a tetrahedron very close to that. First the lower level sets $\{d \leq \epsilon\}$ start with 4 balls, $\chi = 4$; next these balls connect in the 6 centers of the edges P_iP_j , $\chi = 4 - 6 = -2$. In each of the faces there is a ‘hole’ to the interior; each ball is directly connected with all the other balls. After that the ‘hole’ in the center of each face is filled by a 2-cell, $\chi = -2 + 4 = 2$. This happens in the 4 centers of the circumcircles of the face-triangles. There is still a ‘hole’ in the middle, bounded by a component of a level set, which is a topological 2-sphere’. Next one add a 3-cell in this hole (at the center of the circumsphere of the tetrahedron. $\chi = 2 - 1 = 1$. After this there are no more changes in the topology and the lower level sets fills the whole \mathbb{A}^3 . About the critical points:

index 0 at the 4 vertices,

index 1 at the 6 midpoints of the edges,

index 2 at the 4 centers of the circumcircle

index 3 at the center of the circumsphere.

$$\mu_0 - \mu_1 + \mu_2 - \mu_3 = 4 - 6 + 4 - 1 = 1.$$

Next let the tetrahedron exist of an equilateral triangle and a fourth point very near to the center of the circumsphere, but not in the plane of the triangle. The lower level sets $\{d \leq \epsilon\}$ start again with 4 balls, $\chi = 4$; next the 3 balls consecutive connect with the central ball to a 'tree', $\chi = 4 - 3 = 1$. After that there are no more changes in the topology and the lower level set fills the whole \mathbb{A}^3 . About the critical points:

index 0 at the 4 vertices,

index 1 at the 3 midpoints of 3 edges,

no points of index 2,

no points of index 3.

$$\mu_0 - \mu_1 + \mu_2 - \mu_3 = 4 - 3 + 0 - 0 = 1.$$

These are two extreme cases, it is not difficult to notice that there are several other cases with 4 points.

Also in the n -dimensional case there is defined a Delaunay cell-decomposition where points of \mathcal{P} determine a k -cell if their Voronoi cells meet in a $n - k$ -dimensional face. These are dual cell complexes.

For the existence of critical points of the function D it seems to be important if the Delaunay face cuts its 'dual' Voronoi face in its interior, in a boundary point or not.

References

- [Au] F. Aurenhammer, *Voronoi Diagrams - A Survey of a Fundamental Geometric Data Structure*, ACM Computing Surveys, Vol 23, p 345- 405 (1991).
- [Bl] D. W. Blackett, *Elementary Topology*, Academic Press, 1982.
- [Ed] H. Edelsbrunner, *Algorithms in Combinatorial Geometry*, EATCS, Monographs on Computer Science, Volume 10, Springer Verlag 1987.
- [GS] K. R. Gabriel, R. R. Sokal, *A new statistical approach to geographic variation analysis*, Syst. Zoology 18, p 259-278 (1969).
- [Go] A. Goddijn, *communication during a course on Concrete Geometry, Utrecht, 1995*
- [GM] M. Goresky, R. MacPherson, *Stratified Morse Theory*, Ergebnisse der Mathematik und ihrer Grenzgebiete; 3. Folge, Bd 14, Springer Verlag, 1987.
- [Hi] M. W. Hirsch, *Differential topology*, Graduate Texts in Mathematics, Vol 33, Springer Verlag, 1976.
- [Lay] S. R. Lay, *Convex Sets and Their Applications*, Wiley, New York 1972.
- [LS] D. Leven, M. Sharir, *Planning a Purely Translational Motion for a Convex Object in Two-Dimensional Space Using Generalized Voronoi Diagrams*, Discrete Comput. Geometry 2; p 9-31 (1987).

- [Mi] J. Milnor, *Morse Theory*, Annals of Mathematics Studies 51, Princeton University Press 1963.
- [OBS] A. Okabe, B. Boots, K. Sugihara, *Spatial Tesselations, Concepts and Applications of Voronoi Diagrams*, Wiley series in probability and mathematical statistics, 1992.
- [Ur] R. Urquhart, *Graph theoretical clustering based on limited neighborhood sets*, Pattern Recognition 15, p 173-187 .
- [VFOR] J. Vleugels, V. Ferrucci, M. Overmars, A. Rao, *Hunting Voronoi Vertices*, Computational Geometry: Theory and Applications (to appear).

Dirk Siersma,
Department of Mathematics University Utrecht
P.O. Box 80.010, 3508 TA Utrecht, The Netherlands
email: siersma@math.ruu.nl

june 28, 1996

Talk delivered at the Symposium on 'Discrete and Computational Geometry' in honour of M. Sharir at the occasion of his doctorate honourous causa at Utrecht University, March 1996